

pH-Gated Permeability of Variably Charged Species through Polyelectrolyte Multilayer Membranes

Hassan H. Rmaile, Tarek R. Farhat,[†] and Joseph B. Schlenoff*

Department of Chemistry and Biochemistry, Center for Materials Research and Technology (MARTECH),
The Florida State University, Tallahassee, Florida 32306-4390

Received: July 3, 2003; In Final Form: September 4, 2003

The transport of weak acid/base molecules through ultrathin films of polyelectrolyte complex formed by the multilayering method was measured by electrochemical means. The net flux of probe molecule through multilayers is a linear combination of all forms in which that probe is found. Neutral molecules are able to traverse the membrane faster because they rely on nonspecific hopping, whereas charged molecules require extrinsically charged sites, which are doped into the multilayer by external salt. Control over probe charge by external pH is thus an effective way to influence net membrane transport. Flux was simulated by Monte Carlo methods and by analytical expressions, which showed that the pH-dependent component of flux was essentially mirrored by the solution titration curve of the weak acid. In situ attenuated total internal reflection Fourier transform IR measurements revealed that multilayer probe concentration was independent of both the solution salt concentration and state of ionization.

Introduction

Ultrathin films of polyelectrolyte complex, prepared by the layer-by-layer sequential assembly technique,^{1–4} have proven useful for a variety of applications.^{5–11} Some of the most promising uses of these polyelectrolyte “multilayers” (PEMUs) are in the area of analytical^{12–14} and membrane separations.^{14–24} The latter, based on kinetic and thermodynamic (partitioning) factors, is effective for separating enantiomers,¹⁴ ions,^{15–22} neutral molecules,^{23,24} and gases.^{25–27}

Our recent work,^{14,28,29} coordinating theory and experiment to address the membrane transport of solution species in particular, has focused principally on the role of solution ionic strength, which is known to control permeation through PEMUs.^{15a,19} Since the nascent polyelectrolyte complexes employed herein contain minimal “salt” counterions for ion exchange,^{29–31} they are unable to transmit charged species. The addition of salt to the external solution contacting the multilayer reversibly swells or “dopes” the PEMU, converting it from an intrinsic, counterion-free to an extrinsic, ion-containing, and ion-conducting state.²⁹ There are many other strategies, in addition to salt swelling, some reversible and some irreversible, that produce extrinsic charge within PEMUs. For example, internal charge balance may be manipulated by electrochemical methods,³¹ by templating PEMUs with strongly interacting counterions as they are assembled,¹⁶ or by elimination of charged groups.^{17,31}

For multilayers comprising weak acid/base polyelectrolytes, extrinsic charge may be created by protonation/deprotonation under the influence of solution pH.^{15,32} However, these PEMU transformations occasionally trigger phase separations, leading to microporous^{33a,34} and nanoporous materials,^{33b} which, though useful in their own right as novel filtration media, lack the

homogeneity needed for ion separations. An alternative to modulation of PEMU charge is to use the same acid/base chemistry to control the state of charge of permeating molecules instead while employing a pH-independent PEMU. Specifically, neutral molecules do not require extrinsic charge within multilayers to provide sites for ion exchange and ion hopping.²⁹ If a charged species is converted to a neutral one by simple acid/base transformations it is thus possible to enhance considerably the permeability of this species. In the present work, we report the effectiveness of this strategy, using L-ascorbic acid and 3–3(3,4-dihydroxyphenyl)-L-alanine (L-DOPA) as electrochemically active membrane transport probes with ionizable functional groups. Overall membrane flux is further shown to stem from a quasilinear combination of site-specific hopping transport attributable to ionized probe and nonspecific transport of neutral probe.

Experimental Section

Reagents and Materials. Poly(diallyldimethylammonium chloride), PDADMAC (molecular weight, MW, ca. 400 000), and poly(styrenesulfonic acid), PSS (MW ca. 70 000), L-ascorbic acid, and L-DOPA, all from Sigma-Aldrich, were used as received. Sodium chloride and hydrogen potassium phosphate were from Fisher, and potassium ferricyanide was from Mallinckrodt. Solution and mean ion activities were calculated from their corresponding concentrations and appropriate activity coefficients.³⁵ Deionized water (Barnstead, E-pure, Milli-Q) was used to prepare all aqueous solutions.

Methods. The permeability and selectivity of multilayers were studied using redox electrochemical methods. Electrochemical measurements were done using a 100-mL electrochemical cell equipped with a water jacket thermostated to 22 ± 0.1 °C, a platinum counter electrode, and a KCl-saturated calomel electrode (SCE), against which all potentials are quoted. The working electrode was a rotating platinum disk (RDE, from Pine Instruments), 8 mm diameter, mounted in a Pine ASR2 rotator and speed controller. All solutions were deoxygenated

* Author to whom correspondence may be addressed. E-mail: schlen@chem.fsu.edu.

[†] Current address: Department of Chemical Engineering, Massachusetts Institute of Technology, Boston, MA 02139.

with argon prior to electrochemical measurements. Potential ramps were generated by an EG&G Princeton Applied Research 273 potentiostat interfaced to a computer. The electrode was polished with 0.05- μm alumina (Buehler), sonicated, and rinsed in water. The electrode was further sonicated in a mercaptoethanesulfonic acid (MES) solution before deposition to maintain a negatively charged surface. Sequential adsorption of polyelectrolytes onto the rotating disk electrode (RDE) at 300 rpm was performed with the aid of a robot (StratoSequence V, nanoStrata, Inc.). The two-polymer deposition solutions contained 10 mM (based on the polymer repeat unit) polyelectrolyte, 10 mM phosphate buffer solutions (pH = 7.4), and 0.25 M NaCl. Between alternating exposures to the polyelectrolytes, there were three rinses in 10 mM phosphate buffer with no NaCl added. Rinse and polymer solutions were approximately 50 mL each. The deposition time for each layer was 5 min, and each rinse was done for 30 s. The last (anionic) layer was deposited from a solution containing 10 mM of polymer in 10 mM NaCl for 24 h to allow adsorption with minimal surface charge overcompensation.^{28,29} The coated electrode was rinsed and dried. All ascorbic acid and DOPA redox probe solutions were freshly prepared for each electrochemical run at different salt concentrations, since their aqueous solutions are susceptible to air oxidation. The concentration of redox probe was 1 mM for all electrochemical studies. Supporting salt concentrations for electrochemistry were in the range of 0.1–2.0 M NaCl. Flux measurements were obtained using steady-state RDE voltammetry.³⁶

Thicknesses were measured with a Gaertner Scientific L116B Autogain ellipsometer with 632.8-nm radiation at 70° incident angle. A refractive index of 1.54 was employed for the multilayers. Thickness measurements were confirmed using atomic force microscopy (Nanoscope 4, Digital Instruments).³⁷

The concentrations of L-ascorbic acid inside the multilayer, both at low and high pH, were studied using attenuated total reflectance Fourier transform infrared (ATR-FTIR) spectroscopy.²⁹ ATR measurements were performed with a Nicolet Nexus 470 FTIR fitted with a 0.5 mL capacity flow-through ATR assembly housing a 70 \times 10 \times 6 mm 45° germanium crystal (Specac Benchmark). The crystal was cleaned using 50:50 v/v ethanol/H₂O in saturated salt solution. Multilayers were deposited on the ATR crystal while it was loaded in the flow cell by passing polyelectrolyte and rinse solutions, in an alternating manner, through the cell. Twelve layers each of PSS and PDADMAC were deposited using 10 mM polymer in 1 M NaCl also containing 10 mM phosphate buffer (pH = 7.4). The layer-by-layer buildup was monitored using the area of the sulfonate peak at 1033 cm⁻¹. All spectra were recorded using 32 scans and 4 cm⁻¹ resolution. Once the multilayer was built, solutions of 1 mM L-ascorbic acid, at either low (1.8) or high (7.4) pH, were passed one at a time through the ATR flow cell to monitor their concentrations in situ inside the multilayer using one of their characteristic peaks at 1650 cm⁻¹. The spectrum of the final multilayer with buffer solution in the flow cell was used as a background. The salt concentration was varied from 0.2 to 0.8 M NaCl. Ascorbic acid (1 mM) did not show any signal when passed through the uncoated flow cell. To calibrate instrument response, 0.1 M solutions of ascorbic acid, or ascorbate, and 0.1 M poly(styrene sulfonate) were also passed through the uncoated cell.

Results and Discussions

Ion Permeability. The probe ions used in permeability studies, depicted in Figure 1, are electrochemically active weak

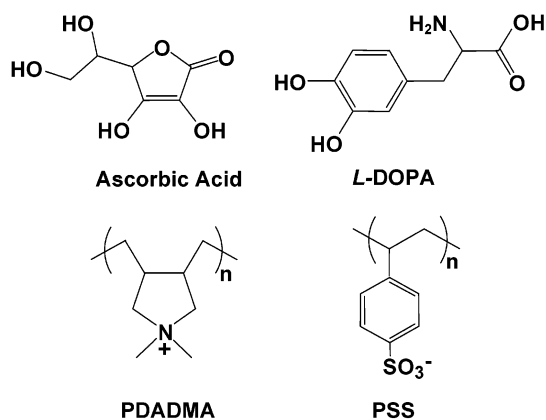


Figure 1. Structures of polyelectrolytes and pH-dependent probe ions used.

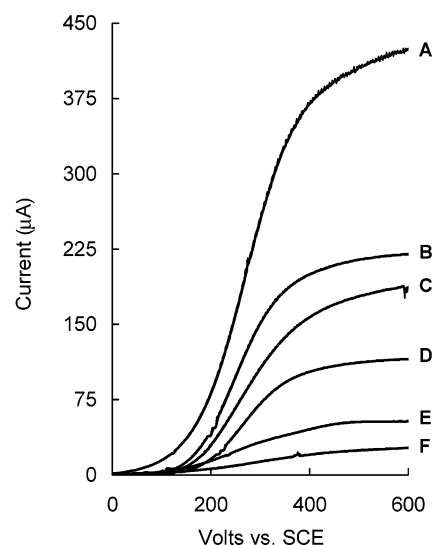


Figure 2. Linear scan voltammograms (LSVs) on a rotating disk electrode: (A) uncoated for L-ascorbic acid; (B) coated at pH = 2.0; (C) coated at pH = 4.0; (D) coated at pH = 5.0; (E) coated at pH = 6.0; (F) coated at pH = 8.0. All solutions were 1 mM ascorbic acid, 0.2 M NaCl. pH was adjusted with buffer solutions or by addition of strong acid/base. Electrode was 8 mm diameter Pt, temperature 22 \pm 0.1 °C, and rotation rate 1000 rpm. The electrode was coated with eight layer pairs of PSS/PDADMA in 0.25 M NaCl. The last (PSS) layer of 16 was deposited from a solution containing 10 mM of polymer in 10 mM NaCl for \sim 24 h to allow adsorption with minimal surface charge overcompensation.²⁹ Note that positive current means oxidation.

acids. Ascorbic acid, AA, has one ionizable functional group, whereas L-DOPA goes from net positive to net neutral (zwitterionic) to net negative charge with increasing pH. The solubility of these probes in aqueous solution remains high and independent of the state of ionization, in contrast to some of the ionizable organic molecules previously evaluated for PEMU permeability, such as ibuprofen.³⁸ The multilayer itself, made from a typical combination of quaternary ammonium and sulfonate polyelectrolytes, remains unaffected by pH changes of the magnitude employed here.³⁹

Linear scan voltammetry of probe ions at the rotating disk is shown in Figure 2 for bare and coated electrodes. Scans approach the ideal S shape, with a plateau current from steady-state convection–diffusion. Redox current is a direct, accurate, and precise measure of the transmembrane flux.³⁶ By use of current from bare electrodes, the series resistance to mass transport through a layer of stagnant liquid adjacent to the electrode may be precisely removed to yield diffusion-limited fluxes through the membrane itself (termed “membrane cur-

rent").²⁸ In Figure 2, the ionic strength of the AA electrolyte is maintained approximately constant with the addition of 0.2 M NaCl and the pH of the 0.01 M phosphate buffer is adjusted over the range pH 8.0 to 2.0 with the addition of acid. It is clear that, all other variables held constant, the membrane permeability of ascorbic acid is much greater at low pH, where it is in the neutral, associated form, than at higher pH, where it is ionized.

For reproducible membrane flux, it is essential to define both the pH and the solution salt concentration. The latter parameter introduces polyelectrolyte segments paired by salt counterions (extrinsic sites) for intersite hopping of charged species. We have termed such a system a "reluctant" exchanger, where bulk ion exchange sites, both cationic and anionic, are forced into the PEMU as a result of external salt concentration.²⁸ This type of exchanger contrasts with the more traditional Donnan type, where ions of opposite charge to the exchanger are included and like-charged ions are excluded. Bulk Donnan exchanging behavior is expected if the multilayer has a preponderance of quasipersistent extrinsic charge.^{16,17,40} Since a layer of extrinsic charge, responsible for sustaining the layer-by-layer growth of PEMUs, exists at the surface, one may observe a contribution from Donnan inclusion to the multilayer ion population for surface charge opposite to that of the probe.^{28,29} In this work, the multilayer was terminated with a thin layer of polyelectrolyte of the same charge as that of the probe ion, minimizing Donnan inclusion.²⁹

An equilibrium treatment of multilayer doping by salt, showing that doping level was proportional to external salt concentration (activity),²⁸ was confirmed by in situ attenuated total reflection Fourier transform infrared (ATR-FTIR) experiments.²⁹ Since the hopping probability for a single charged ion is proportional to the doping level,²⁹ a linear relationship between flux and salt concentration is expected. Such a relationship is observed in Figure 3, where membrane current density is plotted as a function of salt concentration for a variety of solution pH values. Figure 3 clearly shows transport of the single-charge type at extremes of high pH, corresponding to fully ionized probe, and approaches the salt-independent behavior expected for neutral molecules at the low pH extreme. For example, with a solution pK_a of 4.17,⁴¹ ascorbic acid is 99.99% ionized at a pH of 8.0 and thus the current density reflects transport of ascorbate (-1) ion, with a linear slope and intercept at $i_{\text{membrane}} \sim 0 \mu\text{A}$. Conversely, at a pH of 2.0, where ascorbic acid is 99% neutral, the current has a very weak dependence on salt concentration, approaching the expected independent behavior for uncharged species.

Similar control of flux by pH and salt is observed with L-DOPA (Figure 4). At pH = 2.5, L-DOPA has a single positive charge and current exhibits the expected proportionality to salt. At a pH of 8.0, the molecule contains two opposite charges. Ions bearing charge ν exhibit unusual PEMU transport behavior in response to salt; the flux scales with salt ν . This unique feature of ion transport through reluctant exchangers results from a requirement for coincidence, or clustering, of at least ν extrinsic charges before an ion of charge ν can hop.²⁹ From Figure 4 it is evident that the zwitterionic form of L-DOPA behaves as though it were a neutral molecule that does not interact with charged extrinsic sites within the PEMU. In other words, when it is a zwitterion, the charge on L-DOPA is compensated internally, rather than by charged polyelectrolyte segments, probably because of the same entropic reasons that the zwitterion form has no counterions in solution or as a solid. Raising the pH further to 10.8 yields L-DOPA in the -1 form and the

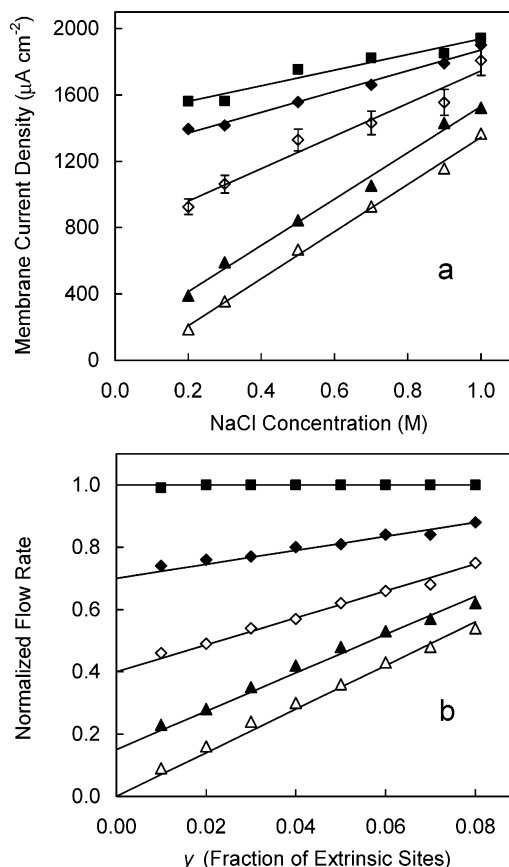


Figure 3. (a) Membrane current density vs salt concentration for 1 mM AA in 10.0 mM phosphate buffer at (i) pH = 2.0 (■), (ii) pH = 3.9 (◆), (iii) pH = 5.1 (◇), (iv) pH = 6.0 (▲), and (v) pH = 8.0 (△). Eight layer pairs of PSS/PDADMA, thickness $560 \pm 50 \text{ \AA}$. Rotation rate of 1000 rpm. $T = 22 \pm 0.1 \text{ }^\circ\text{C}$. Typical error bars are shown on one of the curves. (b) Monte Carlo simulations to illustrate the normalized flow of ascorbic acid as the pH changes. Hopping length is 1 lattice unit, 2D array is 400×500 , probe ion population = 5000. $\bar{\alpha} = 0.01$ mimics a neutral ascorbic acid molecule (corresponding to pH = 2.2, ■) and so on for $\bar{\alpha} = 0.30$ (pH = 3.8, ◆), $\bar{\alpha} = 0.60$ (pH = 4.4, ◇), $\bar{\alpha} = 0.85$ (pH = 4.9, ▲), and $\bar{\alpha} = 0.99$ (pH = 6.2, △). Solid lines are fits to eq 11. Hopping probability, P , for singly charged ascorbate ion is proportional to the doping level, γ , using the empirical formula $P = \gamma/0.14$.

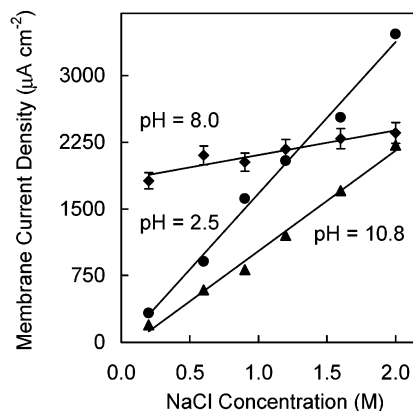


Figure 4. Membrane current density of L-DOPA vs salt concentrations at three different pH values using eight layer pairs of PSS/PDADMA as described in Figure 2. Typical error bars are shown on one of the curves.

concomitant proportionality of current to salt concentration. The flux for the $+1$ form is greater than for the -1 form because

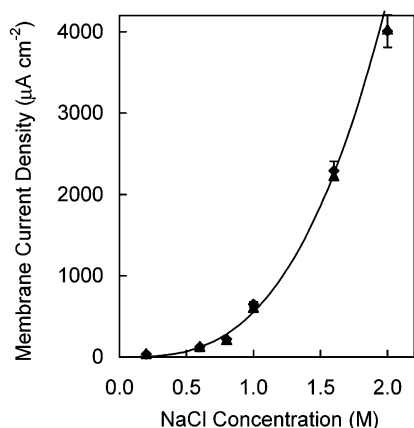


Figure 5. Membrane current density for 1 mM ferricyanide through eight layer pairs of PSS/PDADMA at low (▲) and high pH (◆) showing identical permeation behavior at both pH. Conditions are as in Figure 2.

the membrane concentration of positive L-DOPA is enhanced by Donnan inclusion into the multilayer surface (negative, PSS layer).

To eliminate any possibility that the PSS/PDADMA multilayer was undergoing unforeseen pH-induced changes in morphology or charge, the transport of ferricyanide ion, an ion with nominally pH-independent charge, was evaluated. The flux of ferricyanide through the PEMU, depicted in Figure 5, follows the $[\text{NaCl}]^3$ power law dependence on salt, but does not change as a function of pH.

Mixed Transport Mechanism. Referring to Figure 3, it appears that between extremes of pH, where ascorbic acid is found in either charged or neutral form, intermediate behavior exists, characteristic of contributions from both forms. A diagnostic of such intermediate behavior is a nonzero intercept on the y axis, implying that even when there are no extrinsic reluctant exchanger sites, some ascorbic acid is able, in neutral form, to traverse the PEMU.

Before proceeding to a quantitative analysis, we address the disposition of AA at the molecular level. Ascorbate ion must reside near a positively charged polyelectrolyte segment (extrinsic charge). Undissociated ascorbic acid, on the other hand, partitions into the water volume between polyelectrolyte molecules (the PSS/PDADMA multilayer contains about 50 volume % of water).⁴² The respective differences in location of charged vs neutral AA are akin to the difference between lattice and interstitial sites in solid-state chemistry (although the “lattice” in PEMUs is amorphous), the former is substitutional. The slight increase in flux of neutral molecules with salt seen in Figure 3, and observed previously,²⁹ may be due to an increase in the proportion of water brought in with the salt ions.

A significant finding, predicted by equilibrium considerations of PEMUs, is that the multilayer concentration of charged probe ion is *independent* of salt-doping level.²⁹ Thus, differences in flux for charged species are due to differences in the hopping rate or the diffusion coefficient. Ascorbic acid is found, at any instant, within the solution or multilayer, in either protonated or unprotonated form, the ratio being given by the acid dissociation constant, $\text{p}\bar{K}_a$.

Note that terms relating to multilayer constants or quantities are indicated by a bar. It is assumed that there is a dynamic flux between forms



and that the rates of protonation/deprotonation are slower than the time the ion spends in transit from one site to another (like the Franck–Condon approximation for electronic transitions). The total flux, J_T , is a linear combination of the flux from neutral, HA, and charged, A^- , forms of ascorbic acid

$$J_T = J_{\text{A}^-} + J_{\text{HA}} \quad (2)$$

The total flux can be modeled by a Monte Carlo approach, which has previously been presented in detail.²⁹ In short, a rectangular lattice of defined size is set up (here the array size is 400×500) and populated randomly with extrinsic sites. A more dilute population of probe ions is added, which, on each simulation cycle, attempts to hop in any direction with a defined hopping length. For charged ions, if the destination site contains one of the randomly placed extrinsic sites, the attempt is successful. Neutral molecules hop on every attempt. Net flow rates in any direction under a concentration gradient can be simulated by removing probe ions from one side of the lattice and feeding them in to the other side. The parameter $\bar{\alpha}$ represents the fraction of ascorbic acid in the *dissociated* (charged) form and $1 - \bar{\alpha}$ provides the balance in neutral form where

$$\text{p}\bar{H} = \text{p}\bar{K}_a + \log \frac{\bar{\alpha}}{1 - \bar{\alpha}} \quad (3)$$

A final relationship needed for comparison of parts a (experimental) and b (simulation) of Figure 3 is the doping level, y , as a function of salt concentration. Employing $y = [\text{NaCl}]/12$ for doping of PSS/PDADMA by NaCl,⁴³ the x axes may be aligned as in Figure 3. Using values of $\bar{\alpha}$ that correspond to the pH (eq 3) and assuming $\text{p}\bar{K}_a$ to be 4.17, the normalized Monte Carlo flow rates (Figure 3) exhibit similar scaling to the experimental fluxes.⁴⁴

Analytical expressions for the scaling of flux with salt may be derived starting with a fundamental equation describing flux of species j through a membrane where the concentration of j is zero on one side (as is the case at the limiting current plateau for the hydrodynamic electrochemical system used here) and fixed on the other side⁴⁵

$$J_j = \frac{\bar{D}_j \bar{C}_j}{d} \quad (4)$$

where J_j , \bar{D}_j , \bar{C}_j , and d represent the flux of a species j , its diffusion coefficient through the membrane, its concentration inside the membrane, and the thickness of the membrane, respectively.

The membrane diffusion coefficient for a three-dimensional system is given by⁴⁶

$$D_j = \frac{\delta_j^2 k_{\text{hop},j}}{6} \quad (5)$$

where δ is the average hopping distance and $k_{\text{hop},j}$ is the hopping frequency. The flux contribution from associated ascorbic acid is thus

$$J_{\text{HA}} = \frac{\delta_{\text{HA}}^2 k_{0,\text{hop,HA}} \bar{C}_{\text{HA}}}{6d} \quad (6)$$

where the hopping frequency has been replaced by a hopping *attempt* frequency, $k_{0,\text{hop}}$. In the present work, a hopping attempt is defined as one that is sufficiently energetic to be successful if an unoccupied site is available. For HA, these sites are plentiful and independent of salt. All hopping attempts will be

TABLE 1: Multilayer Concentration of Ascorbic Acid in Terms of Molar Ratio of Ascorbic Acid/PSS Inside the Multilayer^a

[NaCl] (M)	mole ratio AA/PSS ($\times 10^{-4}$)	
	pH = 1.80	pH = 7.40
0.20 M	7.40	7.07
0.40 M	7.53	7.21
0.80 M	7.80	7.42

^a Solution concentration of AA was 1 mM. The precision of the measurement was $\pm 2\%$.

successful. The flux due to ascorbate ion is

$$J_{A^-} = \frac{\delta_{A^-}^2 k_{0,hop,A} P \bar{C}_{A^-}}{6d} \quad (7)$$

Note that eq 7 contains a probability term, P , that is a function of doping level and ion charge.²⁹ Defining

$$\bar{C}_{asc} = \bar{C}_{HA} + \bar{C}_{A^-} \quad (8)$$

and since $\bar{C}_{A^-} = \bar{\alpha} \bar{C}_{asc}$, and substituting eqs 6 and 7 into eq 2, we obtain

$$J_T = \frac{(\delta_{A^-}^2 k_{0,hop,A} P \bar{\alpha} + \delta_{HA}^2 k_{0,hop,HA} (1 - \bar{\alpha})) \bar{C}_{asc}}{6d} \quad (9)$$

Assuming that

$$\delta_{A^-}^2 k_{0,hop,A} = \delta_{HA}^2 k_{0,hop,HA} = \delta_{asc}^2 k_{0,hop,asc} \quad (10)$$

Then eq 9 will simplify to the following

$$J_T = \frac{\delta_{asc}^2 k_{0,hop,asc} \bar{C}_{asc} (P \bar{\alpha} + 1 - \bar{\alpha})}{6d} \quad (11)$$

Three assumptions are made in the preceding. The first is that the membrane concentrations of AA in either form do not change with salt concentration. While \bar{C} of charged species has been shown to be independent of salt concentration, it has previously only been assumed that \bar{C} of neutral species are unaffected by salt concentration. The second, related, assumption is that the multilayer exhibits no significant preference for either HA or A^- . If there were a difference in partitioning of either species into the PEMU, then \bar{C}_{asc} would change as a function of $\bar{\alpha}$. Experiments with ATR-FTIR, using PSS/PDADMA multilayers coated on germanium ATR crystals, as described previously,²⁹ were performed for AA solutions at different pH and salt concentration. The results, summarized in Table 1, are given in terms of molar ratios of AA to sulfonate group, using the sulfonate as a convenient internal standard. This approach eliminates differences in relative signal due to swelling and refractive index changes. To obtain absolute AA concentration, the molar concentration of PSS can be estimated (ca. 2 M) and multiplied by the AA/PSS molar ratio. The PEMU concentrations of both HA and A^- were indeed found to be independent of both pH and salt concentration. The fact that the partitioning of a species into a PEMU is independent of its charge, another remarkable characteristic of polyelectrolyte multilayers, supports the two assumptions made above. The third assumption, given directly by eq 10, is supported by the finding that at high salt concentrations the flux from A^- approaches that from HA (see the pH = 8.0 and pH = 2.0 curves in Figure 3).

The straightforward linear combination of fluxes (eq 11) is used in Figure 3b to model the flux scaling at different pH. A

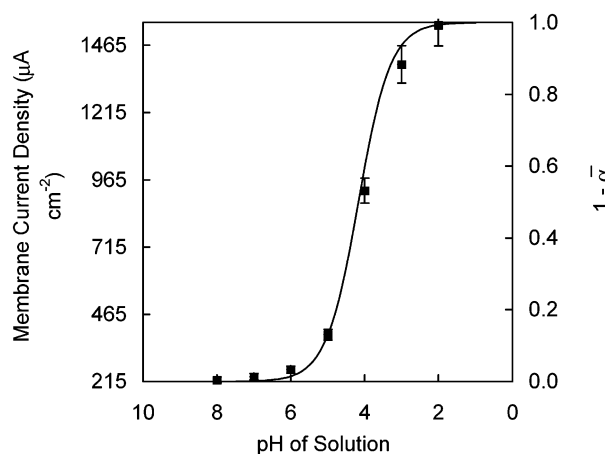


Figure 6. Membrane current density of ascorbic acid (left axis) vs the pH of the solution determined experimentally at 0.2 M NaCl [■]. The PEMU film is eight layer pairs of PSS/PDADMA. Conditions are as in Figure 2. The right axis corresponds to the solid line and represents a fit according to eq 15 where $r = 1.0$. It is normalized so that the lowest current represents full dissociation and the highest current represents full protonation. Typical error bars are shown.

dependence of hopping probability on doping is required, and the relationship $P = y/0.14$ produces a satisfactory fit.

Acid Dissociation Constant, \bar{K}_a , of Ascorbic Acid inside the PEMU. Although protons are able to enter the multilayer, the pH is easily controlled and defined for the solution only. Yet the relevant parameters for AA transport are PEMU quantities. The partition coefficients of ascorbic acid molecules, Q_{HA} , and ascorbate, Q_{A^-} , between the PEMU and solution are defined as

$$Q_{HA} = \frac{\bar{C}_{HA}}{C_{HA}} = \frac{1 - \bar{\alpha}}{1 - \alpha} \quad (12)$$

and

$$Q_{A^-} = \frac{\bar{C}_{A^-}}{C_{A^-}} = \frac{\bar{\alpha}}{\alpha} \quad (13)$$

Therefore using eqs 1, 12, and 13, the acid dissociation constant inside the PEMU film \bar{K}_a is

$$\bar{K}_a = \frac{\bar{\alpha} C_{H^+} Q_{HA}}{1 - \bar{\alpha} Q_{A^-}} \quad (14)$$

Rearranging eq 14 yields a modified Henderson–Hasselbalch equation where

$$\text{pH} = \text{p}\bar{K}_a + \log r \left(\frac{\bar{\alpha}}{1 - \bar{\alpha}} \right) \quad (15)$$

where

$$r = \frac{Q_{HA}}{Q_{A^-}}$$

A plot of membrane current at different solution pH, with constant ionic strength, is shown in Figure 6. Assuming the lowest and highest current values represent the extremes of pH-dependent current, eq 15 may be used to fit the data. The curve, essentially representing the titration of AA inside the PEMU, shows a satisfactory fit for $r = 1$, indicating no preference by the multilayer for AA between neutral or ionized form, in agreement with the direct ATR-FTIR measurements. Another

interesting finding was that a good fit was obtained with $pK_a = pK_a = 4.17$. Evidently, the pK_a of the probe ion is not modified by interaction with the multilayer, in contrast to the multilayer polymers themselves.⁴⁷ This is because an A^- ion entering the multilayer does not break an energetically favorable polymer/polymer ion pair; instead, it replaces a relatively weakly interacting chloride ion.

Conclusions

The facile, reversible control of flux through PEMUs has significant implications for membrane transport, and drug loading and release in particular. The strategy of using pH changes to modify the charge of a molecule, and thereby influence permeability, is generally applicable to small and large molecules. For example, a small change in pH for a (macro)-molecule bearing multiple weak acid functionalities may have a significant impact on the permeability of this molecule through a PEMU. Bioactive agents transported in PEMU capsules^{48,49} may be released more quickly in acidic or basic environments. For example, an amine-bearing drug molecule should be released more quickly in the intestine (higher pH) than in the stomach (lower pH) since it is neutral in the former and charged (protonated) in the latter. A straightforward model describing membrane transport by hopping, limited by the density of available sites, rationalizes the behavior of the small, hydrophilic molecules. The success of the model depends on the fact that the probe molecules do not undergo significant changes in size on ionization. Larger, more hydrophobic molecules would probably exhibit slower hopping frequencies.

Acknowledgment. The authors gratefully acknowledge support from the National Science Foundation (DMR 9727717) and the donors of the Petroleum Research Fund.

References and Notes

- (1) Decher, G.; Schlenoff, J. B.; Lehn, J. *Multilayer Thin Films: Sequential Assembly of Nanocomposite Materials*; Wiley-VCH: Cambridge, 2003.
- (2) Decher, G. *Science* **1997**, *277*, 1232.
- (3) Arys, X.; Jonas, A. M.; Laschewsky, A.; Legras, R. In *Supramolecular Polymers*; Ciferri, A., Ed.; Marcel Dekker: New York, 2000; pp 505–564.
- (4) Decher, G.; Hong, J. D.; Schmitt, J. *Thin Solid Films* **1992**, *210*, 831.
- (5) Fou, A. C.; Onitsuka, O.; Ferreira, M.; Rubner, M. F.; Hsieh, B. R. *J. Appl. Phys.* **1996**, *79*, 7501.
- (6) (a) Decher, G.; Lehr, B.; Lowack, K.; Lvov, Y.; Schmitt, J. *Biosens. Bioelectron.* **1994**, *9*, 677. (b) Sun, Y.; Zhang, X.; Sun, C.; Wang, B.; Shen, J. *Macromol. Chem. Phys.* **1996**, *197*, 147.
- (7) (a) Onda, M.; Lvov, Y.; Ariga, K.; Kunitake, T. *Biotech. Bioeng.* **1996**, *51*, 163. (b) Lvov, Y. M.; Lu, Z.; Schenkman, J. B.; Rusling, J. F. *J. Am. Chem. Soc.* **1998**, *120*, 4073.
- (8) (a) Laurent, D.; Schlenoff, J. B. *Langmuir* **1997**, *13*, 1552. (b) Stepp, J.; Schlenoff, J. B. *J. Electrochem. Soc.* **1997**, *144*, L155.
- (9) Cheung, J. H.; Fou, A. F.; Rubner, M. F. *Thin Solid Films* **1994**, *244*, 985.
- (10) (a) Hammond, P. T.; Whitesides, G. M. *Macromolecules* **1995**, *28*, 7569. (b) Huck, W. T. S.; Yan, L.; Stroock, A.; Haag, R.; Whitesides, G. M. *Langmuir* **1999**, *15*, 6862.
- (11) Farhat, T. R.; Schlenoff, J. B. *Electrochem. Solid State* **2002**, *5*, B13.
- (12) Graul, T. W.; Schlenoff, J. B. *Anal. Chem.* **1999**, *71*, 4007.
- (13) Kapnissi, C. P.; Akbay, C.; Schlenoff, J. B.; Warner, I. M. *Anal. Chem.* **2002**, *74*, 2328.
- (14) Rmaile, H. H.; Schlenoff, J. B. *J. Am. Chem. Soc.* **2003**, *125*, 6602.
- (15) (a) Harris, J. J.; Bruening, M. L. *Langmuir* **2000**, *16*, 2006. (b) Sukhorukov, G. B.; Antipov, A. A.; Voigt, A.; Donath, E.; Möhwald, H. *Macromol. Rapid Commun.* **2001**, *22*, 44.
- (16) Balachandra, A. M.; Dai, J. H.; Bruening, M. L. *Macromolecules* **2002**, *35*, 3171.
- (17) Dai, J. H.; Balachandra, A. M.; Lee, J. I.; Bruening, M. L. *Macromolecules* **2002**, *35*, 3164.
- (18) Sullivan, M. D.; Bruening, M. L. *J. Am. Chem. Soc.* **2001**, *123*, 11805.
- (19) Krasemann, L.; Tieke, B. *Langmuir* **2000**, *16*, 287.
- (20) Jin, W.; Toutianoush, A.; Tieke, B. *Langmuir* **2003**, *19*, 2550.
- (21) Han, S.; Sethson, B. L. *Electrochim. Acta* **1999**, *45*, 845.
- (22) Klitzing, R. V.; Möhwald, H. *Macromolecules* **1996**, *29*, 6901.
- (23) Meier-Haack, J.; Lenk, W.; Lehmann, D.; Lunkwitz, K. J. *Membr. Sci.* **2001**, *184*, 233.
- (24) Krasemann, T.; Toutianoush, A.; Tieke, B. *J. Membr. Sci.* **2001**, *181*, 221.
- (25) Stroeve, P.; Vasquez, V.; Coelho, M. A. N.; Rabolt, J. F. *Thin Solid Films* **1996**, *284*, 708.
- (26) Levasalmi, J.; McCarthy, T. J. *Macromolecules* **1997**, *30*, 1752.
- (27) Sullivan, D. M.; Bruening, M. L. *Chem. Mater.* **2003**, *15*, 281.
- (28) Farhat, T. R.; Schlenoff, J. B. *Langmuir* **2001**, *17*, 1184.
- (29) Farhat, T. R.; Schlenoff, J. B. *J. Am. Chem. Soc.* **2003**, *125*, 4627.
- (30) Michaels, A. S. *Ind. Eng. Chem.* **1965**, *57*, 32.
- (31) Schlenoff, J. B.; Ly, H.; Li, M. *J. Am. Chem. Soc.* **1998**, *120*, 7626.
- (32) Shiratori, S. S.; Rubner, M. F. *Macromolecules* **2000**, *33*, 4213.
- (33) (a) Mendelsohn, J. D.; Barrett, C. J.; Chan, V. V.; Pal, A. J.; Mayes, A. M.; Rubner, M. F. *Langmuir* **2000**, *16*, 5017. (b) Fery, A.; Scholer, B.; Cassagneau, T.; Caruso, F. *Langmuir* **2001**, *13*, 3779.
- (34) Kim, B. Y.; Bruening, M. L. *Langmuir* **2003**, *19*, 94.
- (35) *Properties of Aqueous Solutions of Electrolytes*; Zaytsev, I. D., Aseyev, G. G., Eds.; CRC press: Boca Raton, 1992.
- (36) (a) Ikeda, T.; Schmehl, R.; Denisevich, P.; Willman, K.; Murray, R. W. *J. Am. Chem. Soc.* **1982**, *104*, 2683. (b) Bard, A. J.; Faulkner, L. R. *Electrochemical Methods*; Wiley: New York, 2002; Chapter 8.
- (37) Rmaile, H. H.; Schlenoff, J. B. *Polym. Mater. Sci. Eng.* **2001**, *84*, 678.
- (38) Qiu, X.; Leporatti, S.; Donath, E.; Möhwald, H. *Langmuir* **2001**, *17*, 5375.
- (39) Rmaile, H. H.; Schlenoff, J. B. *Polym. Mater. Sci. Eng.* **2003**, *88*, 556.
- (40) Calvo, E. J.; Wolosiuk, A. J. *Am. Chem. Soc.* **2002**, *124*, 8490.
- (41) Windholz, M. W.; Budavari, S.; Blumetti, R. F.; Otterbein, E. S. *The Merck Index*; Merck & Co., Inc.: Rahway, NJ, 1983; p 120.
- (42) Farhat, T.; Yassin, G.; Dubas, S. T.; Schlenoff, J. B. *Langmuir* **1999**, *15*, 6621.
- (43) Dubas, S. T.; Schlenoff, J. B. *Langmuir* **2001**, *17*, 7725.
- (44) Farhat, T. R. Ph.D. Dissertation, The Florida State University, 2002.
- (45) Helfferich, F. *Ion Exchange*; McGraw-Hill: New York, 1962; Chapter 8.
- (46) Egelstaff, P. *An Introduction to the Liquid State*; Academic Press Inc.: New York, 1967; Chapter 10, pp 119–132.
- (47) Rmaile, H. H.; Schlenoff, J. B. *Langmuir* **2002**, *18*, 8263.
- (48) Kato, N.; Schuetz, P.; Fery, A.; Caruso, F. *Macromolecules* **2002**, *35*, 9780.
- (49) Khopade, A. J.; Caruso, F. *Biomacromolecules* **2002**, *3*, 1154.